

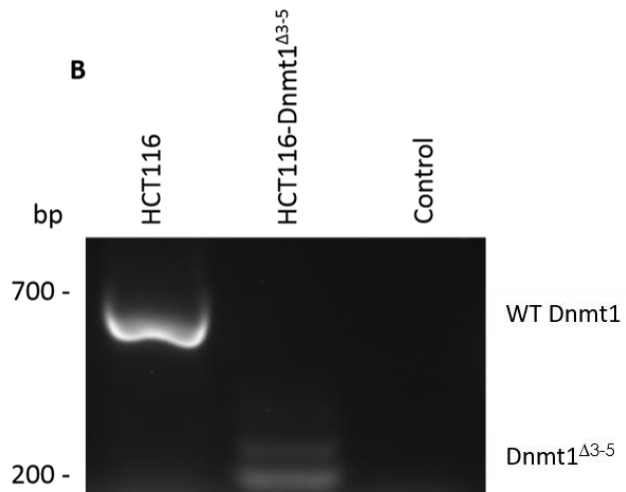
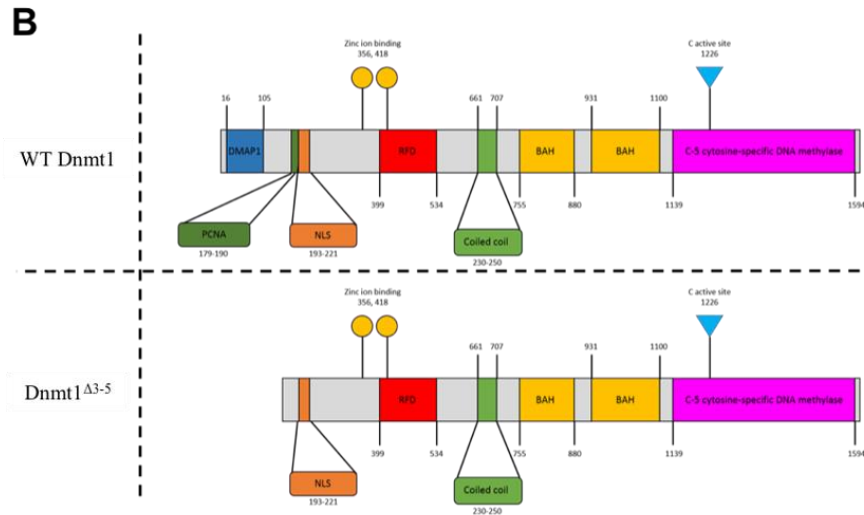
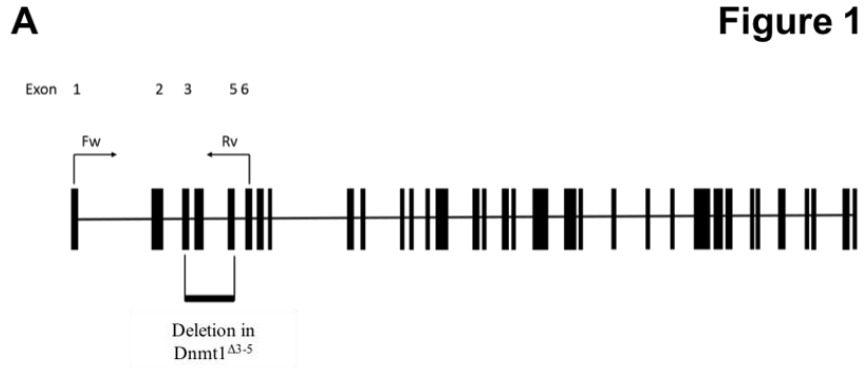
Proteomic analysis of Dnmt1  
hypomorphic colorectal cancer cells  
reveals activation of markers of  
epithelial-mesenchymal transition  
and re-localization of Beta-Catenin

Data from thesis titled;

**Proteomic analysis of Wnt and epigenetic regulatory protein networks in  
colorectal cancer.**

By Emily Hannah Bowler-Barnett

**Figure 1**



**Schematic diagram of Dnmt1 exons and protein domains of HCT116 and HCT116-Dnmt1 $\Delta^{3-5}$  cells.** Exon configuration of WT Dnmt1, with annotation of primer sites used for analysis of Dnmt1 $\Delta^{3-5}$ , and highlighted region of genomic deletion in this cell line. Protein domain schematic based on Pfam sites in Dnmt1 and Dnmt1 $\Delta^{3-5}$ .

**Analysis of genomic Dnmt1 status in HCT116-Dnmt1 $\Delta^{3-5}$  cells.** Polymerase chain reaction analysis of Dnmt1 in HCT116-Dnmt1 $\Delta^{3-5}$  cells in comparison to the endogenous WT gene in HCT116 cells. mRNA was extracted from cells, converted to cDNA by reverse transcription and cDNA analysed by PCR using primers specific to Dnmt1 exons 1 and 6. Control PCR reaction was empty plasmid Pc3DNA construct. PCR products were then analysed by gel electrophoresis resulting in a reduced Dnmt1 product size in HCT116-Dnmt1 $\Delta^{3-5}$  cells, second lighter band in in HCT116-Dnmt1 $\Delta^{3-5}$  cells was due to unspecific binding of primer set, however sequence was still derived from Dnmt1.

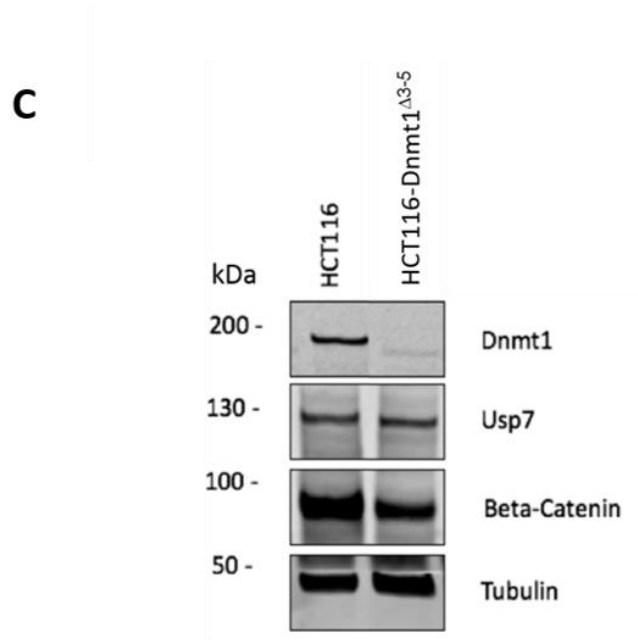
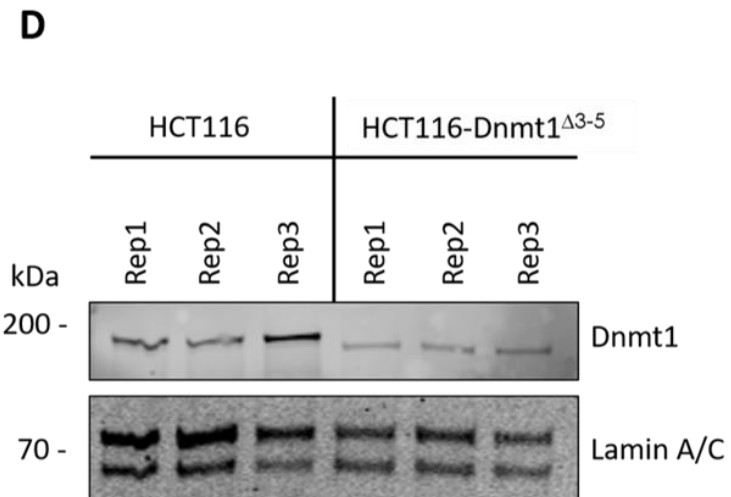


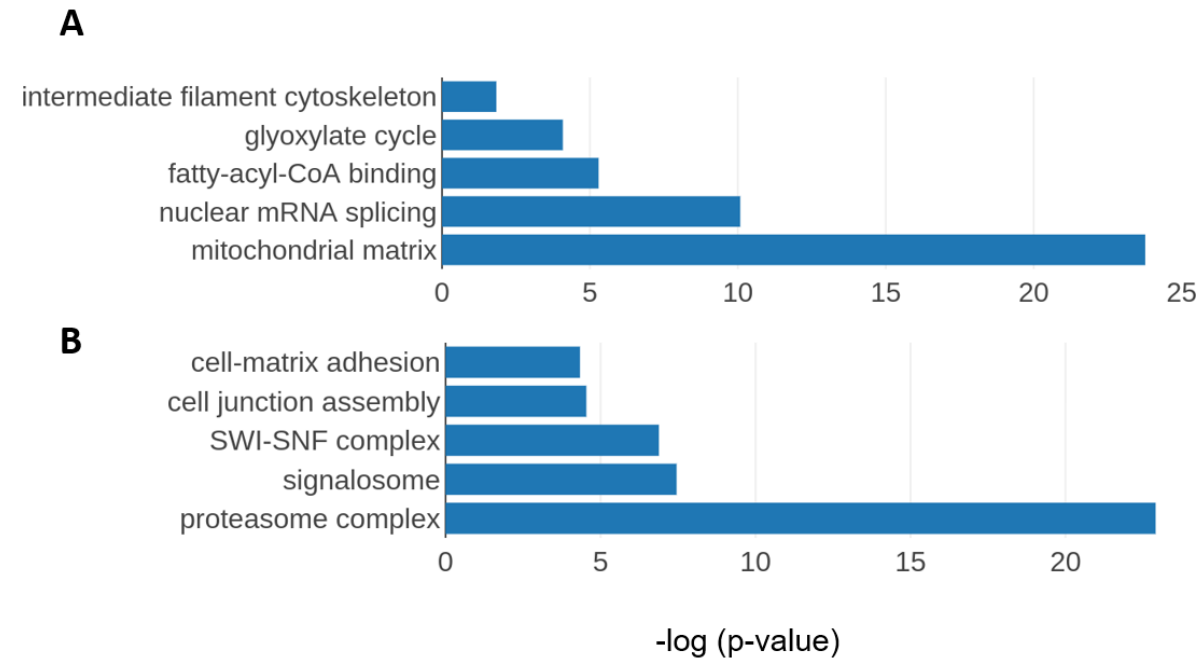
**Figure 1**

**Western blot analysis of Dnmt1 and interaction partners in HCT116 and HCT116-Dnmt1 $\Delta^{3-5}$  cells.** 15 $\mu$ g of whole protein lysates from HCT116 and HCT116-Dnmt1 $\Delta^{3-5}$  cells were loaded onto a single phase 8% SDS gel and analysed by western blot analysis for protein expression of Dnmt1, Usp7, and Beta-Catenin. Tubulin protein abundance was used as a loading control. N=3.



**Nuclear-enriched protein samples of HCT116 and HCT116-Dnmt1 $\Delta^{3-5}$  cells prepared for mass spectrometry analysis of their nuclear proteomic profile.** 15 $\mu$ g of nuclear-enriched protein lysates from HCT116 and HCT116-Dnmt1 $\Delta^{3-5}$  cells, three replicates of each, were loaded onto a single phase 8% SDS gel and analysed by western blot analysis for protein expression of Dnmt1. Lamin A/C protein abundance was used as a loading control for the nuclear-enriched lysate. These samples were then taken forward and prepared for nuclear proteomic analysis by data independent mass spectrometry analysis.

**Figure 2**



**Gene Ontology terms enriched in the proteome from HCT116-Dnmt1<sup>Δ3-5</sup> cells.** Gene Ontology terms from the set of significantly ( $p < 0.05$ ) differentially increased (A) and significantly differentially decreased (B) proteins in hypomorph cells. Selected GO terms where  $p\text{-value} < 0.05$  (t-test with Bonferroni correction) and the rank difference between hypomorph and wild-type GO terms are shown. Results are presented graphically using GraphPad Prism.

C

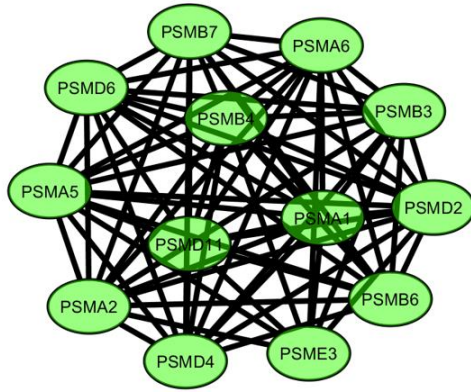
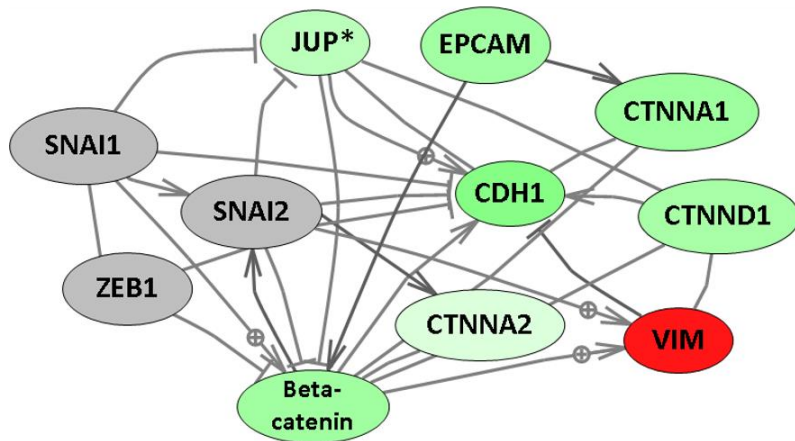


Figure 2

**Proteasome network analysis of proteins with differential abundance in HCT116-Dnmt1<sup>Δ3-5</sup> cells.** Proteasome protein interaction networks were identified using String DB (V10.5), using evidence-based directional interaction search settings. Networks were then extracted and manually pseudo-coloured to articulate differential protein abundance change in the nuclear proteomic profile of HCT116-Dnmt1<sup>Δ3-5</sup> cells using Cytoscape (V3.6.1) String DB app.

D

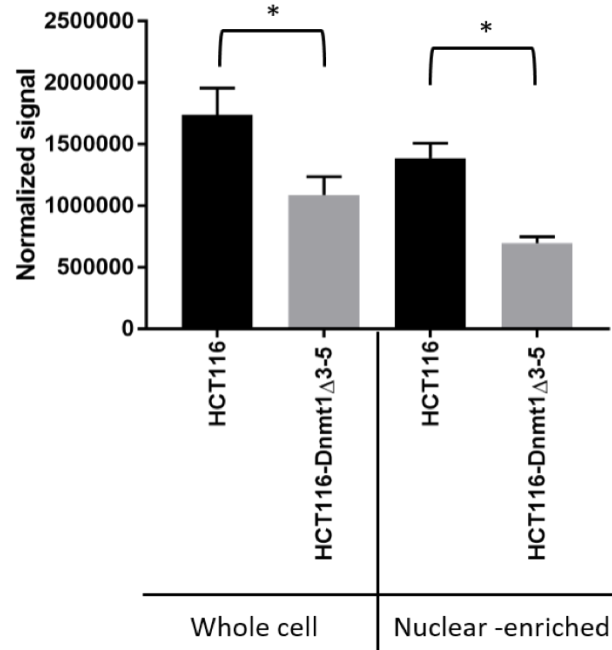


**Catenin-EMT network analysis of proteins with differential abundance in HCT116-Dnmt1<sup>Δ3-5</sup> cells.** Network nodes are coloured according to mutant/wild-type abundance ratio, red = increased abundance, = green decreased abundance. Nodes in grey indicate proteins not identified in the mass spectrometry datasets but analysed by Western blot. Protein interaction networks were identified using Pathway Studio and String DB, using evidence-based directional interaction search settings. Networks were then extracted and manually pseudo-coloured to articulate differential abundance change in the nuclear proteomic profile of HCT116-Dnmt1<sup>Δ3-5</sup> cells. \*= JUP protein abundance not significantly different in the proteomics data.

E

Figure 2

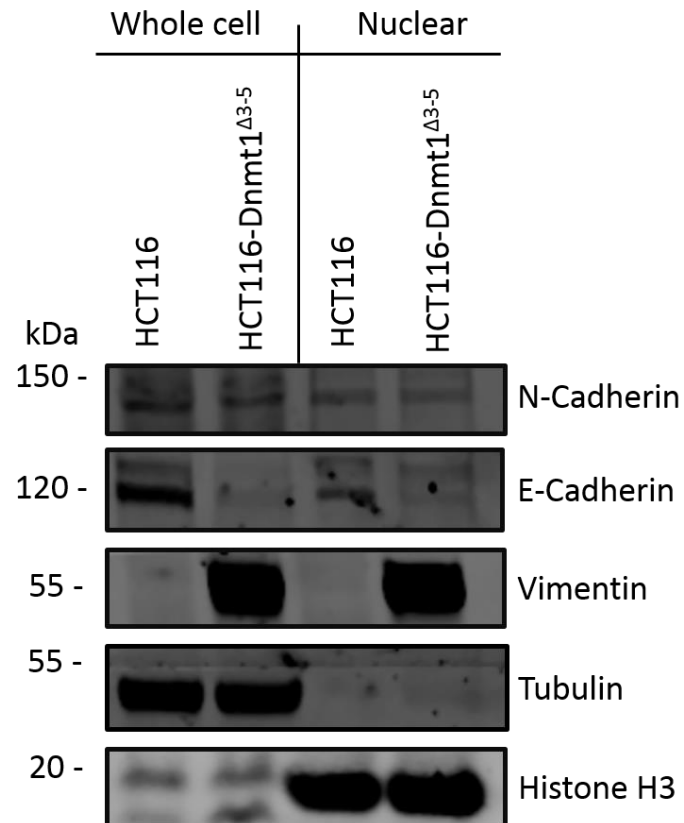
Protein abundance of Delta-Catenin in HCT-Dnmt1<sup>Δ3-5</sup> whole cell and nuclear-enriched protein lysates.



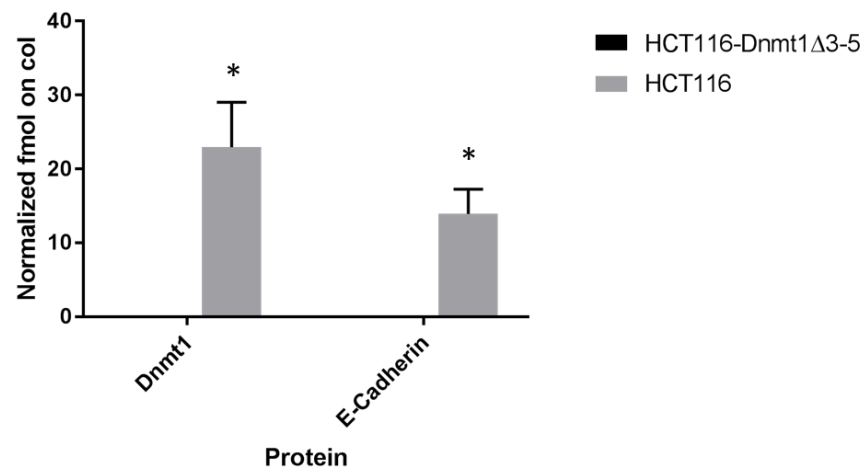
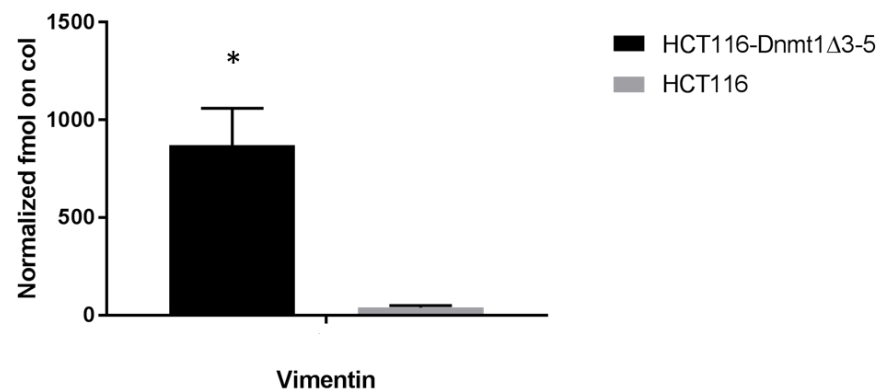
**Graphical analysis of nuclear enriched and whole cell protein lysates for protein abundance of Delta-Catenin.** 15 $\mu$ g of nuclear-enriched or whole cell protein lysates from HCT116 and HCT116-Dnmt1<sup>Δ3-5</sup> cells were loaded onto a single phase 8% SDS gel and analysed by western blot analysis for protein expression of Delta-Catenin.  $\beta$ -Actin protein abundance was used as a loading control for the whole cell protein lysate and Histone H3 protein abundance was used as a loading control for the nuclear-enriched lysate. N=3. Signal was normalized to respective loading controls and plotted graphically (GraphPad Prism) \* = P value <0.05 (Student's t-test)

Figure 3

A



**Analysis of nuclear enriched and whole cell protein lysates for protein abundance of EMT markers.** 15 $\mu$ g of nuclear-enriched or whole cell protein lysates from HCT116 and HCT116-Dnmt1 $\Delta$ 3-5 cells were loaded onto a single phase 8% SDS gel and analysed by western blot analysis for protein expression of Vimentin, N-Cadherin, and E-Cadherin. Tubulin,  $\beta$ -Actin protein abundance was used as a loading control for the whole cell protein lysate and Lamin B1/Histone H3 protein abundance was used as a loading control for the nuclear-enriched lysate. N=3.

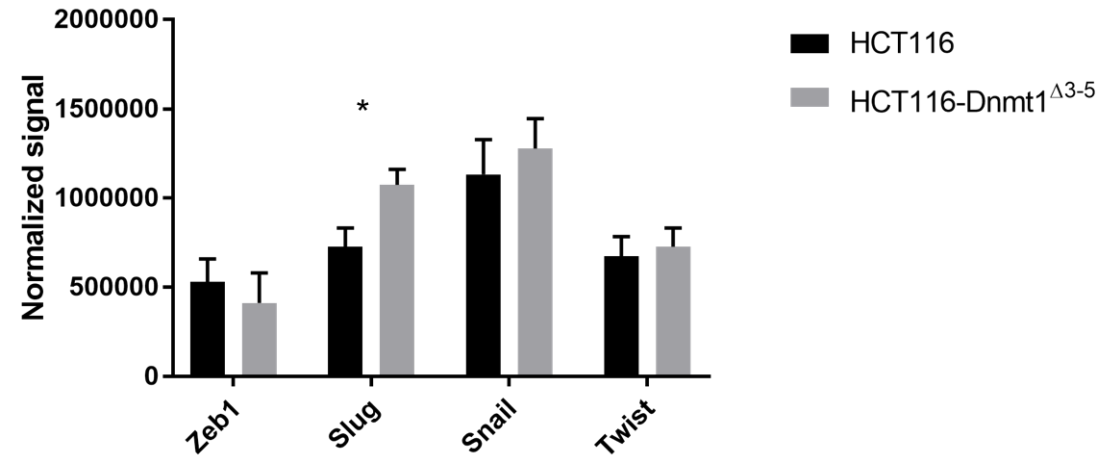
**B****Figure 3****Protein abundance of Dnmt1 and E-Cadherin in nuclear-enriched proteomic profiles****Protein abundance of Vimentin in nuclear-enriched proteomic profiles**

**Mass spectrometry protein quantification of Dnmt1 and key EMT protein markers.** Graphical analysis (GraphPad Prism) of normalized average fmol on column quantification of Dnmt1, Vimentin, and E-Cadherin. N-Cadherin was not identified in the dataset, and Dnmt1 and E-Cadherin were identified only in HCT116 samples. \* = p value <0.05 (Student's t-test adjusted for Benjamini-Hochberg correction).

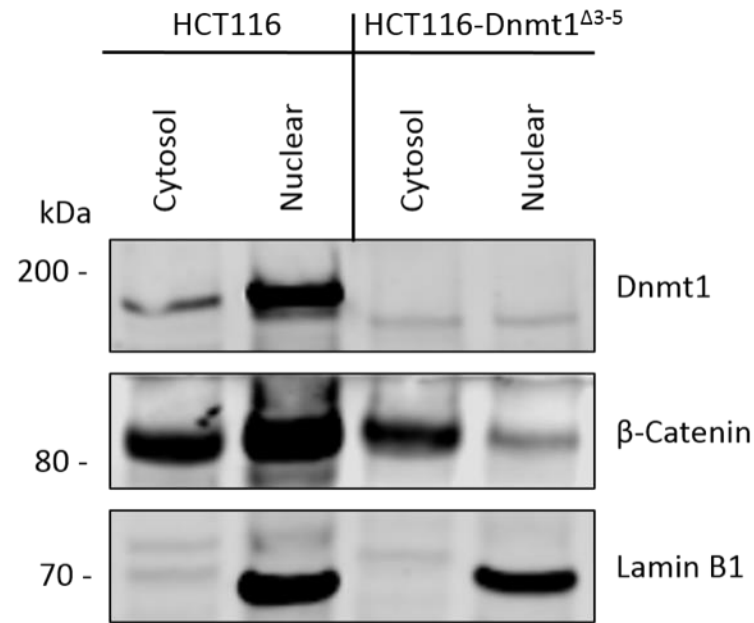
Figure 3

C

Abundance of EMT transcription drivers in  
HCT-Dnmt1 $\Delta^{3-5}$  cells.



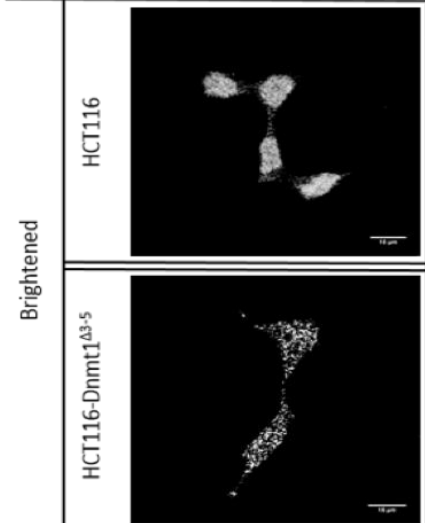
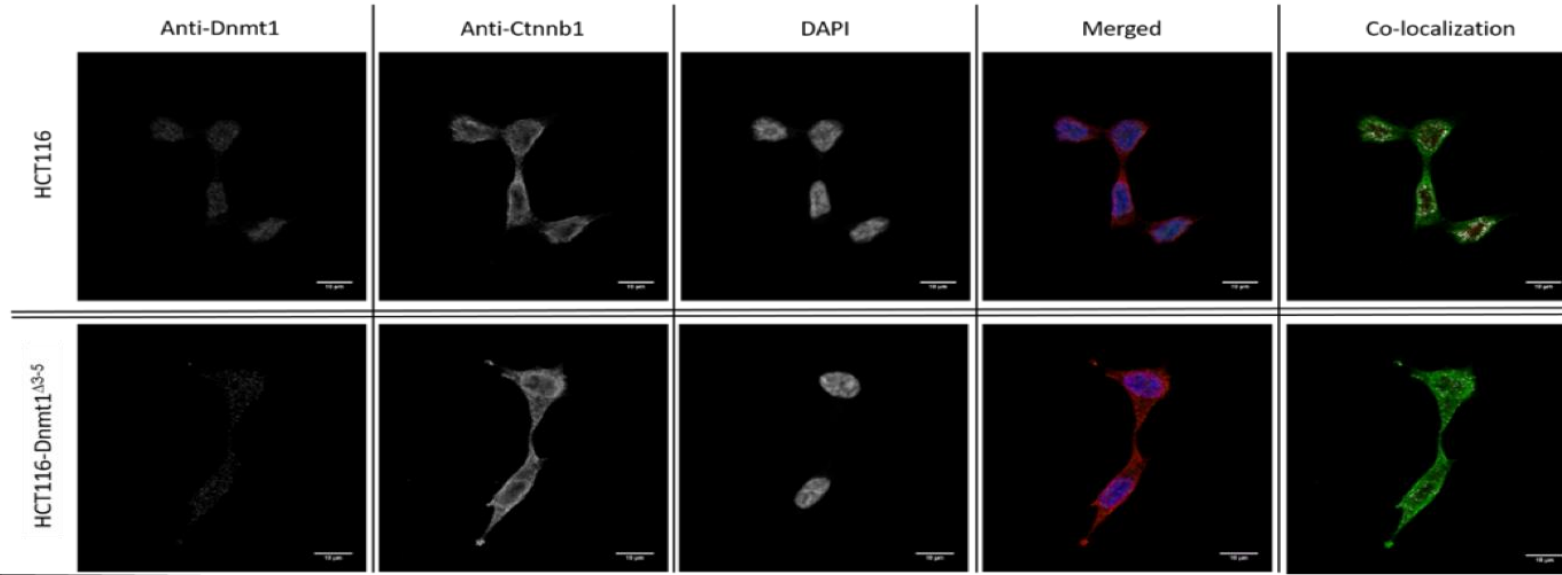
**Western blot analysis of transcriptional drivers of EMT in HCT116-Dnmt1 $\Delta^{3-5}$  cells.** 15 $\mu$ g of nuclear-enriched protein lysates from HCT116 and HCT116-Dnmt1 $\Delta^{3-5}$  cells were loaded onto a single phase 8% SDS gel and analysed by western blot analysis for protein abundance of Dnmt1, Zeb1, Slug, Snail, and Twist. Lamin A protein abundance was used as a loading control. Western blot signal was normalized to loading control and presented graphically using GraphPad Prism. N=3. \* = P value <0.05. (Student's t-test)

**A****Figure 4**

**Analysis of nuclear and cytosolic enriched protein lysates for Dnmt1 and Beta-Catenin localization.** 15 $\mu$ g of nuclear-enriched or cytosol-enriched protein lysates from HCT116 and HCT116-Dnmt1 $\Delta^{3-5}$  cells were loaded onto a single phase 8% SDS gel and analysed by western blot analysis for protein expression of Dnmt1 and Beta-Catenin. Lamin B1 protein abundance was used as a loading control for the nuclear-enriched lysate. N=3.

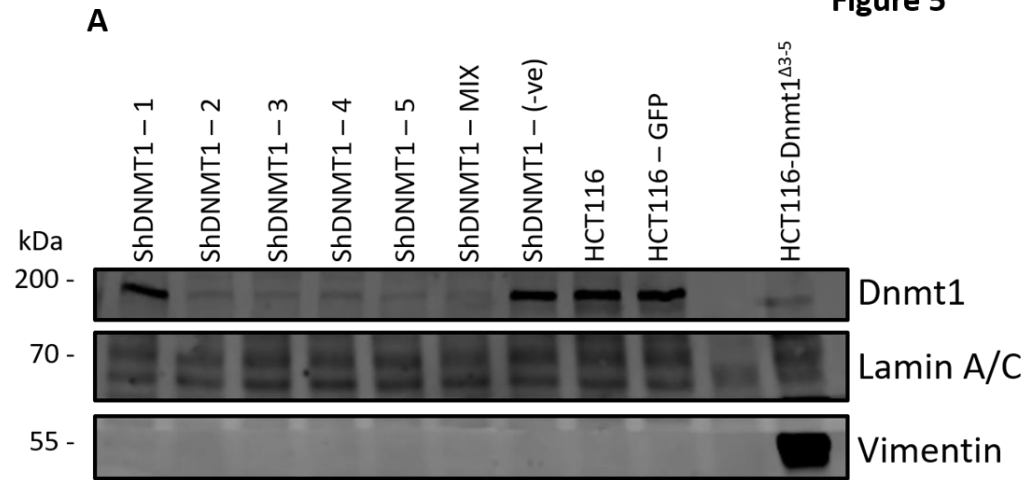
Figure 4

B

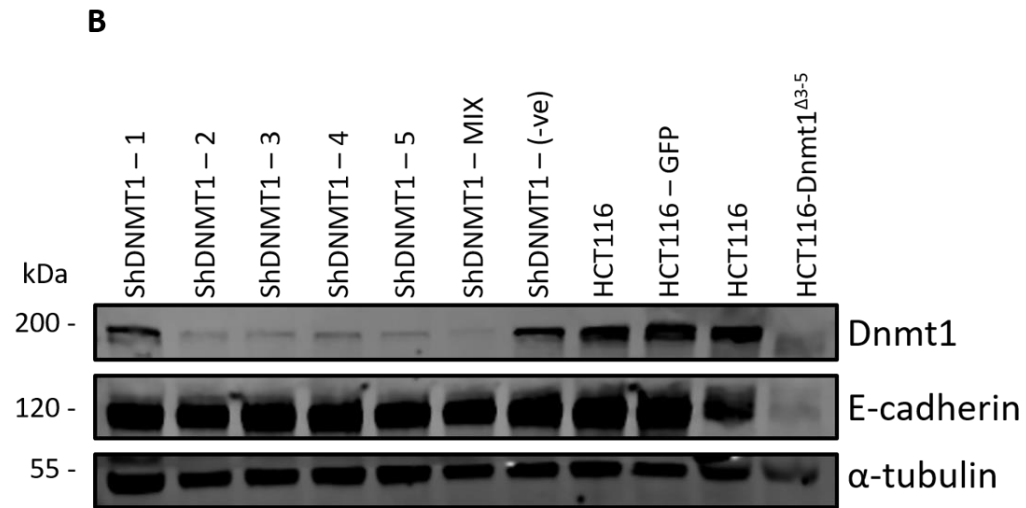


**Immunofluorescence analysis of Beta-Catenin and Dnmt1 localization in HCT116 and HCT116-Dnmt1<sup>Δ3-5</sup> cells.** Localization of Dnmt1 and Beta-Catenin protein was assessed using fluorophore conjugated secondary antibodies and DAPI fixing agent. Channels are presented separately in addition to merged. Co-localization of Dnmt1 and Beta-Catenin was analysed, areas of co-localization of Dnmt1 (red) and Beta-Catenin (green) are highlighted in white. Anti-Dnmt1 antibody images were brightened for image presentation purpose.

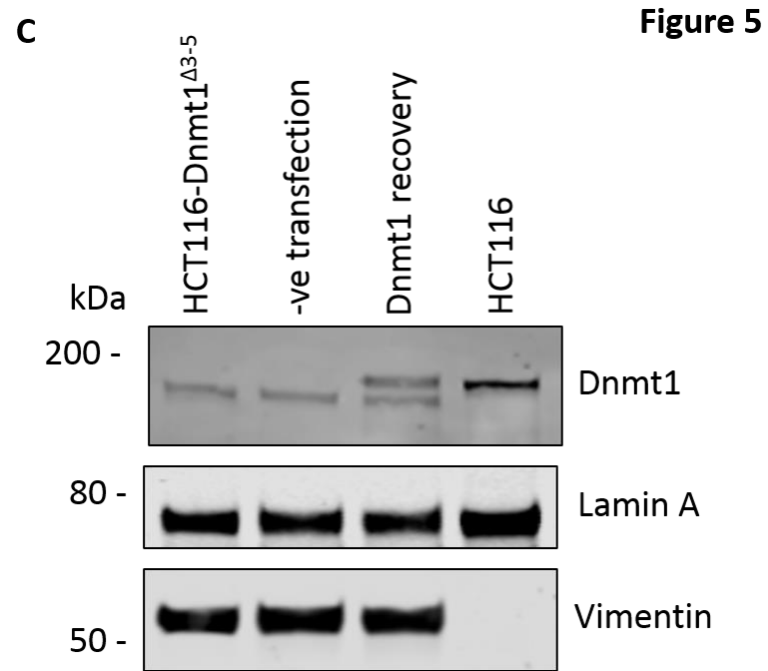
Figure 5



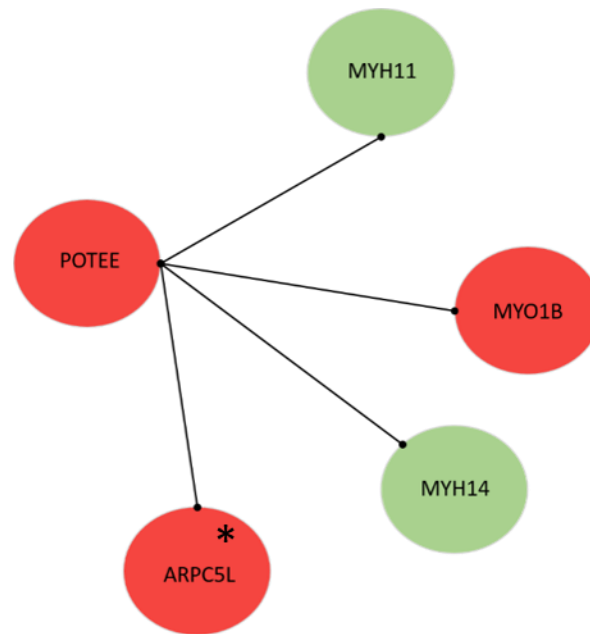
**Dnmt1 shRNA knockdown analysis on Vimentin protein abundance.** 15μg of whole cell protein lysates from shRNA knockdown HCT116 cells, HCT116-GFP controls cells and HCT116-Dnmt1<sup>Δ3-5</sup> cells were loaded onto a single phase 8% SDS gel and analysed by western blot analysis for protein expression of Vimentin. A-Tubulin and Lamin A/C protein abundance were used as a loading control. N=3.



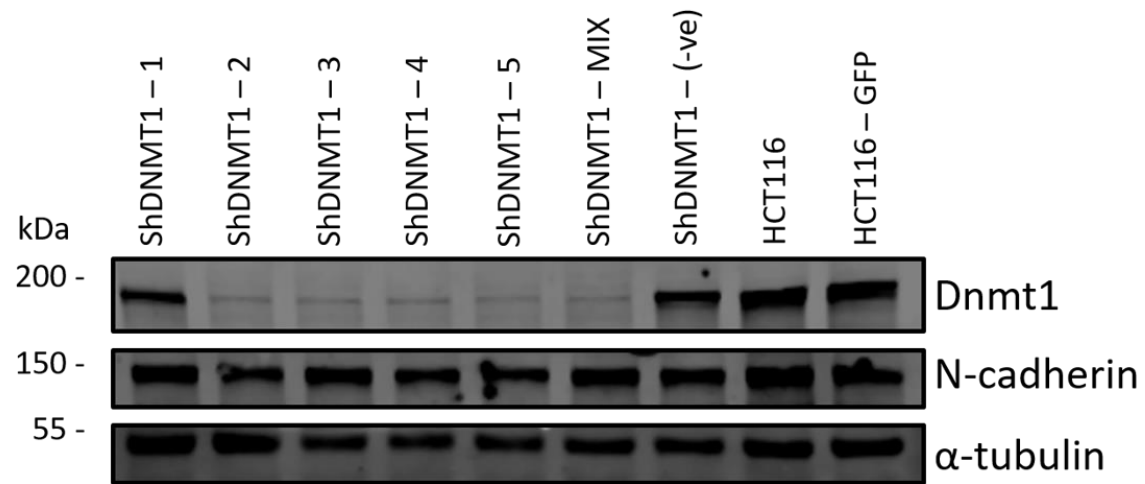
**Dnmt1 shRNA knockdown analysis on E-Cadherin protein abundance.** 15μg of whole cell protein lysates from shRNA knockdown HCT116 cells, HCT116-GFP controls cells and HCT116-Dnmt1<sup>Δ3-5</sup> cells were loaded onto a single phase 8% SDS gel and analysed by western blot analysis for protein expression of E-Cadherin. A-Tubulin protein abundance was used as a loading control. N=3.



**The effect of wild type Dnmt1 protein expression rescue in HCT116-Dnmt1<sup>Δ3-5</sup> cells on Vimentin protein abundance.** 15μg of whole cell protein lysates from HCT116 cells, HCT116-Dnmt1<sup>Δ3-5</sup> cells, and HCT116-Dnmt1<sup>Δ3-5</sup> cells transfected with either a full length WT Dnmt1 expression vector or an empty control were loaded onto a single phase 8% SDS gel and analysed by western blot analysis for protein expression of Dnmt1. Tubulin protein abundance was used as a loading control. N=2.

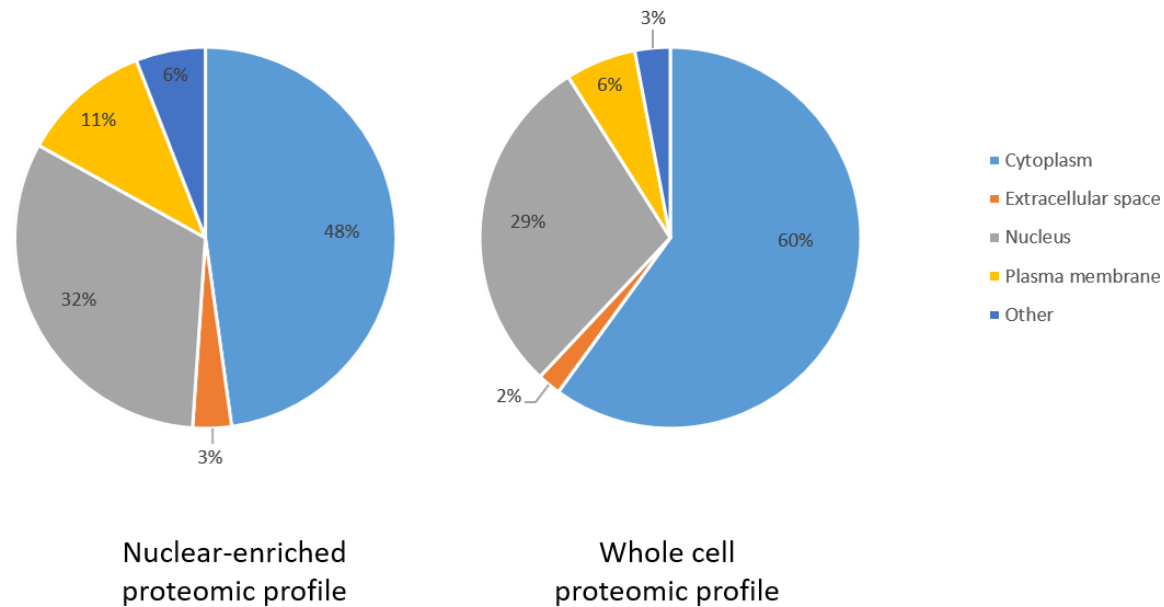


**Cellular architecture network analysis in HCT116-Dnmt1 $\Delta^{3-5}$  cells.** Cellular architecture protein network was identified using String DB (V10.5), using evidence-based directional interaction search settings. Networks were then extracted and manually pseudo-coloured to articulate decreased protein abundance change in the nuclear proteomic profile of HCT116-Dnmt1 $\Delta^{3-5}$  cells. Red = increased. Green = decreased (\* = differential change in abundance is statistically significant <0.05 FDR=5% Benjamini-Hochberg corrected t-test).



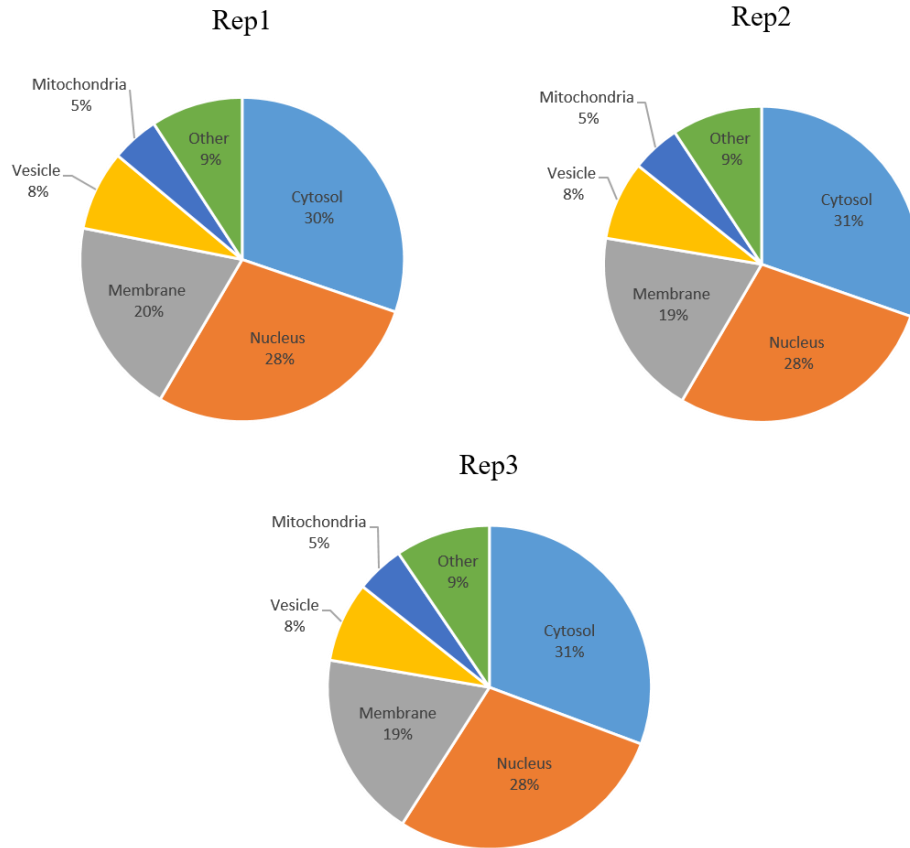
**Dnmt1 shRNA knockdown analysis on N-Cadherin protein abundance.** 15 $\mu$ g of whole cell protein lysates from shRNA knockdown HCT116 cells, HCT116-GFP controls cells and HCT116-Dnmt1 $\Delta^{3-5}$  cells were loaded onto a single phase 8% SDS gel and analysed by western blot analysis for protein expression of N-Cadherin.  $\alpha$ -Tubulin protein abundance was used as a loading control. N=3. Credit; Alex Smith-Vidal.

Cellular compartment enrichment analysis of nuclear-enriched Dnmt1 hypomorph dataset.



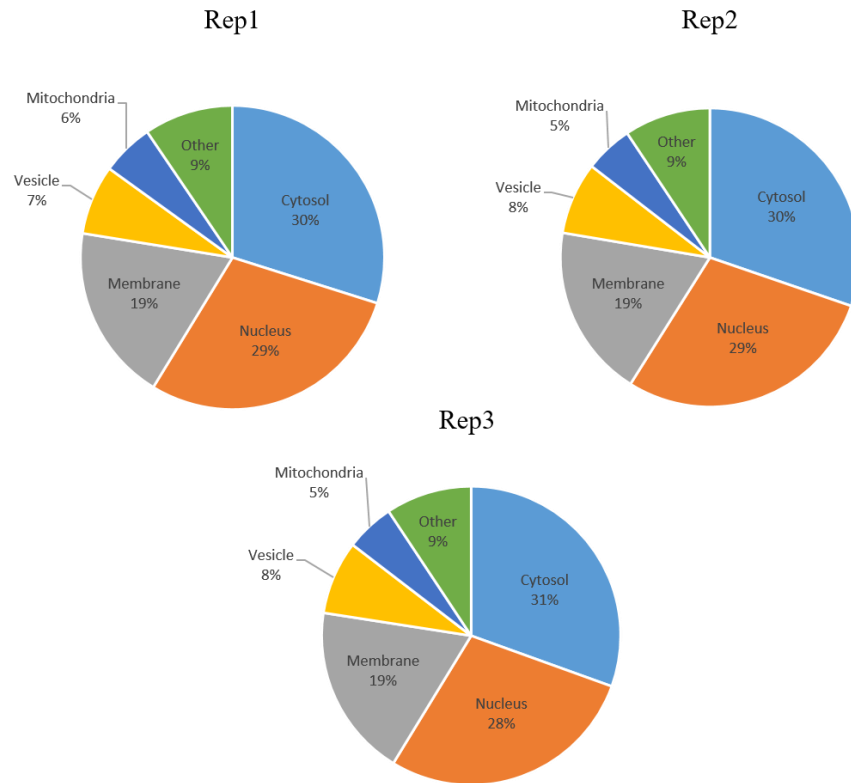
**GO cellular localization enrichment analysis of nuclear-enriched Dnmt1 hypomorph proteomic dataset.** Proteins IDs from Dnmt1 hypomorph proteomic analysis dataset and a comparable whole cell proteomic dataset were searched for their GO localization term using Ingenuity Pathway Analysis (IPA) (QIAGEN). Results were plotted graphically using GraphPad Prism.

Gene ontology cell compartment analysis of nuclear-enriched HCT116 proteomic data.



**Gene ontology analysis of cell compartment enrichment in nuclear-enriched proteomics samples from HCT116 cells.** Total proteins identified in each replicate sample were searched for their cell compartmentalization association using Gene Ontology (Ashburner et al, 2000). Generalized compartments were selected that represented the higher orders of subcellular compartment localization, results were presented as the number of proteins associated with a compartment as a percentage of the total. The category ‘Other’ includes cytoskeleton, ribosome, and endoplasmic reticulum. Results are presented graphically using GraphPad Prism.

Gene ontology cell compartment analysis of nuclear-enriched HCT116-Dnmt1<sup>Δ3-5</sup> proteomic data.



**Gene ontology analysis of cell compartment enrichment in nuclear-enriched proteomics samples from HCT116-Dnmt1<sup>Δ3-5</sup> cells.** Total proteins identified in each replicate sample were searched for their cell compartmentalization association using Gene Ontology (Ashburner et al, 2000). Generalized compartments were selected that represented the higher orders of subcellular compartment localization results were presented as the number of proteins associated with a compartment as a percentage of the total. The category ‘Other’ includes cytoskeleton, ribosome, and endoplasmic reticulum. Results were presented graphically using GraphPad Prism.